AIP ADVANCES **5**, 047131 (2015)

Radiometric calibration of optical microscopy and microspectroscopy apparata over a broad spectral range using a special thin-film luminescence standard

J. Valenta[a] and M. Greben
Faculty of Mathematics and Physics, Department of Chemical Physics & Optics, Charles University, Ke Karlovu 3, 121 16 Prague 2, Czechia

(Received 31 December 2014; accepted 10 April 2015; published online 20 April 2015)

Application capabilities of optical microscopes and microspectroscopes can be considerably enhanced by a proper calibration of their spectral sensitivity. We propose and demonstrate a method of relative and absolute calibration of a microspectroscope over an extraordinary broad spectral range covered by two (parallel) detection branches in visible and near-infrared spectral regions. The key point of the absolute calibration of a relative spectral sensitivity is application of the standard sample formed by a thin layer of Si nanocrystals with stable and efficient photoluminescence. The spectral PL quantum yield and the PL spatial distribution of the standard sample must be characterized by separate experiments. The absolutely calibrated microspectroscope enables to characterize spectral photon emittance of a studied object or even its luminescence quantum yield (QY) if additional knowledge about spatial distribution of emission and about excitance is available. Capabilities of the calibrated microspectroscope are demonstrated by measuring external QY of electroluminescence from a standard poly-Si solar-cell and of photoluminescence of Er-doped Si nanocrystals. © *2015 Author(s). All article content, except where otherwise noted, is licensed under a Creative Commons Attribution 3.0 Unported License.* [http://dx.doi.org/10.1063/1.4918970]

I. INTRODUCTION

Appropriate correction for the spectral response of an experimental apparatus is necessary for any luminescence experiment involving a wide spectral range.[1] The main purpose of such calibration is a correction of spectral-shape distortions and it is most often a *relative calibration* done in "arbitrary units." The *absolute calibration* is only required for special radiometric setups and experiments.[2,3]

Recently, availability of highly-sensitive low-noise CCD cameras and well-corrected spectrographs enabled fast development of various imaging spectroscopes for remote spectroscopy, microspectroscopy etc. The full potential of such devices can be exploited only upon thorough geometrical (imaging) and radiometrical calibration.[4]

Here we describe a straightforward procedure of the absolute calibration of a microscope and/or a microspectroscope over a broad spectral range covering large part of visible (VIS) and near-infrared (NIR) regions. Such a broad range is covered by combining two parallel detection branches – each one consisting of a spectrograph and a 2D-detector array (camera). A key point of our method is exploitation of a luminescing standard sample formed by a thin layer of Si nanocrystals. Finally, two application examples are presented: Electroluminescence (EL) spectroscopy of a silicon solar cell and photoluminescence (PL) quantum yield (QY) measurement of Er-doped Si nanocrystals.

[a]Author to whom correspondence should be addressed. Electronic mail: jan.valenta@mff.cuni.cz

 ©Author(s) 2015

All article content, except where otherwise noted, is licensed under a Creative Commons Attribution 3.0 Unported license. See: http://creativecommons.org/licenses/by/3.0/ Downloaded to IP: 195.113.33.228 On: Mon, 20 Apr 2015 14:08:59

II. EXPERIMENTAL SET-UP

Micro-scopy and -spectroscopy experiments are performed using a specially designed setup (Fig. 1(a)) based on an inverted microscope (Olympus IX-71) with the NIR-optimized objective lens (LMPlan IR 50×/0.55, working distance of 6 mm, focal length f = 3.6 mm). A wide-field excitation is performed in the epifluorescence configuration by a 405-nm diode laser beam whose focal plane is shifted from the sample plane – the circular excited area has diameter of about 94 μm (using the above mentioned objective lens). Laser excitation power in the sample plane is measured by a power meter (Coherent Field Master GS).

Emitted signal is divided by a short-pass dichroic beam-splitter at 1000 nm (Fig. 1(b)). Light with shorter wavelengths (the limits of ~500 - 1000 nm are imposed by the applied dichroic filter) is coupled to a 30-cm imaging spectrograph[5] with a back-thinned LN-cooled CCD camera, while longer wavelengths (> 1000 nm) are detected by a 50-cm imaging spectrograph with an InGaAs camera (the pixel size of both cameras is 20 × 20 μm). In case when the parallel detection in the two spectral regions is not required, the VIS detection branch can be used without the short-pass 1 μm filter, which enlarges the detectable range of this branch to about 350-1100 nm. Magnification factor of both imaging spectrometers is close to 1, therefore the size of an input slit and its image on a camera are equal.

Both the VIS and NIR images (or spectra) of the same sample spot can be acquired simultaneously. Images are obtained using spectrograph gratings turned to zero-order or using a mirror

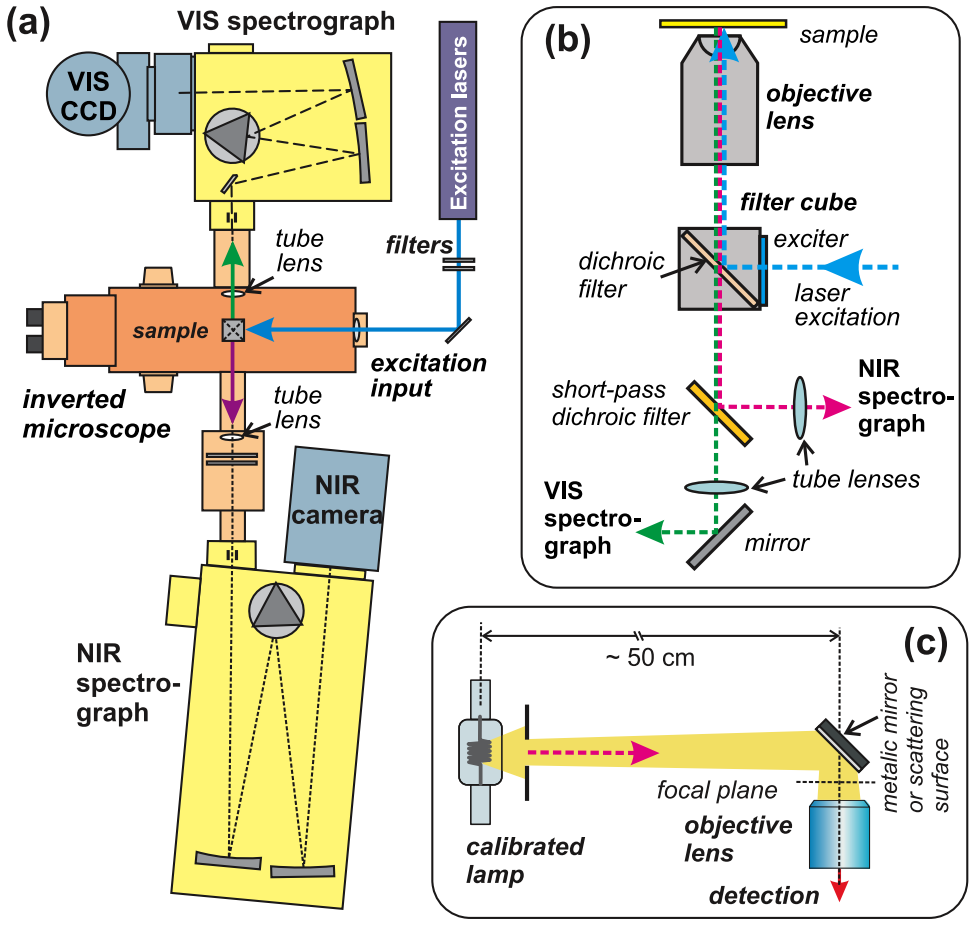

FIG. 1. (a) Top-view scheme of the microspectroscopy set-up based on an inverted optical microscope with two parallel detection branches – visible (VIS) and near-infrared (NIR). Each detection branch consists of an imaging spectrograph and a 2D-detector array (camera). (b) Optical paths in the central part of the microspectroscope (vertical cross-section). (c) Schematical configuration of the sensitivity calibration measurement using a radiance standard (calibrated lamp).

All article content, except where otherwise noted, is licensed under a Creative Commons Attribution 3.0 Unported license. See: http://creativecommons.org/licenses/by/3.0/ Downloaded to IP: 195.113.33.228 On: Mon, 20 Apr 2015 14:08:59

instead of a grating. Imaging magnification (linear) M is measured with a microscale slide giving values of 49× and 58× for VIS and NIR detector, respectively (this is due to different tube lenses with focal length of 18 and 20 cm, respectively). The area for spectral detection is selected by introducing a slit at the input image plane of a spectrometer and detected with a grating turned to a desired central wavelength position.[6] The spatial resolution of this wide-field apparatus is given by the diffraction limit to about $1.1 \times \lambda$, where λ is wavelength of light using for an imaging. The characterization of the apparatus spectral response is described in paragraph III.

Luminescence properties of a standard sample (see paragraph IV.) are characterized by separate devices. Absolute external quantum yield of photoluminescence is determined via a set-up based on an integrating sphere (IS) with diameter of 10 cm (SphereOptics GmbH). A sample is placed inside IS on one removable port in the position opposite to the excitation port where a light-emitting diode (LED) of desirable wavelength is mounted to provide PL excitation. Output signal is collected by a fused-silica fiber bundle whose output is coupled to an imaging spectrometer (Acton SpectraPro SP2150i) with a deep-depletion back-illuminated CCD camera (Spec-10:400B, Princeton Instruments) and a liquid-nitrogen-cooled CCD camera is used for detection. Spectral sensitivity of the complete apparatus is calibrated over a broad spectral range (300-1700 nm) using two radiation standards (Newport Oriel): a 45-W tungsten halogen lamp (above 400 nm) and a deuterium lamp (below 400 nm). The PL QY is calculated as the ratio of the number of emitted photons (the difference between the investigated and the reference sample (i.e. a bare substrate) signals in the region of photoluminescence) and the number of absorbed photons (integrated decrease of the excitation source signal in the sample compared to the reference). More details on the PL QY set-up and the theoretical basis are given in our recent paper.[7]

Spatial distribution of PL is determined via a goniometer set-up. A sample, excited by a diode laser (473 nm) in direction perpendicular to the plane of a luminescing layer, is placed in a center of a rotating stage on which a quartz fiber bundle is mounted and rotated around a sample. The collected PL signal (spatial resolution of about 1°) is detected by the same spectroscope as for PL QY measurements described above. In this way a horizontal cross-section of the spatial distribution of PL is obtained.[8]

III. CALIBRATION OF THE RELATIVE SPECTRAL RESPONSE USING A STANDARD TUNGSTEN LAMP

A calibrated tungsten halogen filament lamp with low power of 45 W (Oriel model No. 63358) is appropriate for microspectroscope calibrations. This lamp is placed at the distance of 50 cm from the objective lens (see Fig. 1(c)) and reflected by a reflectance standard (made from the Spectraflex® material by LabSphere) or a protected aluminium mirror (Thorlabs). The *calibrated spectral irradiance of the standard* ($\Xi_S(\lambda)$ in $W \cdot m^{-2} \cdot nm^{-1}$) is given for the distance of 50 cm but the reflection $R(\lambda)$ and coupling efficiency K modify the input flux actually entering the microscope (K represents a numerical constant - unknown for this moment - equal to the ratio between nominal irradiance and the irradiance actually entering the apparatus).

First, we perform a *relative sensitivity calibration* of the two spectroscope branches taking $(K \cdot \Xi_S \cdot R \cdot a)/(h\nu)$ [photon$\cdot s^{-1} \cdot nm^{-1}$] as an *input spectral photon irradiance* Φ_{in}, where a is the area from which signal is collected and $h\nu$ is photon energy. The spectral sensitivity of an apparatus $C(\lambda)$ (Eq. (1)) is determined as the ratio of the *spectral signal rate* ${S_\lambda}^A$ (the lower index λ discriminates spectral signal given in [counts$\cdot s^{-1} \cdot nm^{-1}$] from the signal rate S^A in [counts$\cdot s^{-1}$]) collected from the image area A and the *input spectral photon irradiance* from the sample area a ${\Phi_{in}}^a$. The sample area a and its image A are related by the imaging magnification M, $a = A/M^2$. We recommend expressing signal in "natural" area units of a 2D detector array (camera), it means *pixels*. Then *signal rate per pixel* S^P is given as $S^A \cdot / A^p$, where A^p is the area of a one pixel (here $20 \times 20\,\mu m^2$). For illustration we provide Fig. 2, where the (spectrally integrated) signal S^p is averaged over 3×2 pixels (white rectangles in Fig. 2). In the *spectral mode*, the signal is integrated in vertical direction (3 pixels) and must be divided by a spectral step Δ_λ in order to correctly represented ${S_\lambda}^p$ in units of [count$\cdot s^{-1} \cdot nm^{-1}$ per pixel]. The minimal spectral step Δ_λ is determined by the dispersion of

All article content, except where otherwise noted, is licensed under a Creative Commons Attribution 3.0 Unported license. See: http://creativecommons.org/licenses/by/3.0/ Downloaded to IP: 195.113.33.228 On: Mon, 20 Apr 2015 14:08:59

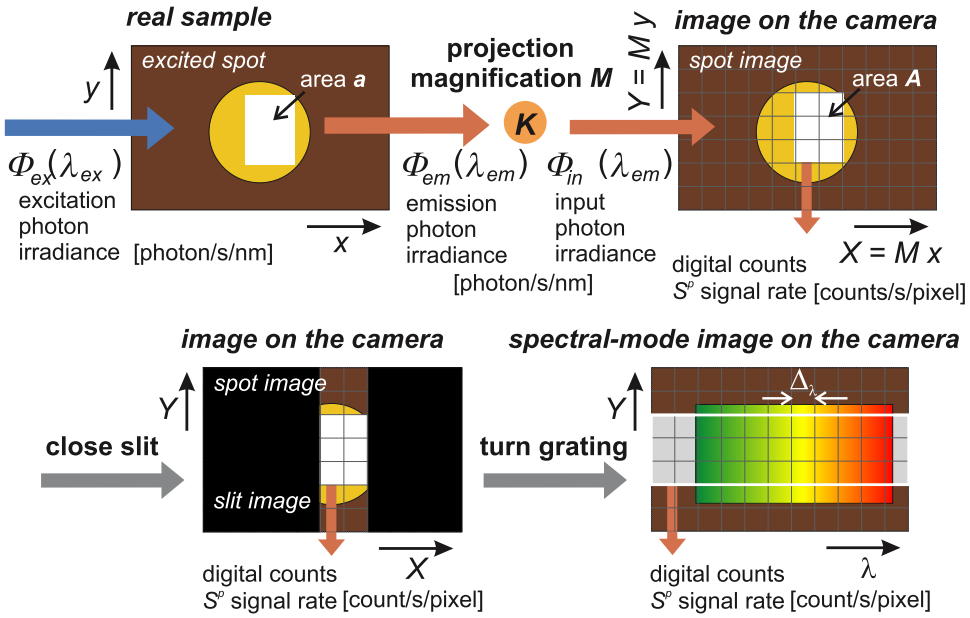

FIG. 2. Relations between the sample, its image and the spectral image and between the input photon irradiance and the detected signal rate.

a spectrometer grating per one detector pixel and the effective spectral step can be increased by binning (integrating) of several pixels along the wavelength axis.

Finally, we obtain the *spectral sensitivity* of the apparatus C_{VIS} and C_{NIR} as

$$C_{VIS/NIR}(\lambda) = \frac{S^A_\lambda\,[count/s/nm]}{\Phi^a_{in}\,[photon/s/nm]} = \frac{S^p(\lambda)\cdot A/(A^p\cdot\Delta_\lambda)}{K\cdot\Xi_S(\lambda)\cdot R(\lambda)\cdot a/h\nu} = \frac{h\nu\cdot S^p(\lambda)\cdot M^2}{K\cdot\Xi_S(\lambda)\cdot R(\lambda)\cdot A^p\cdot\Delta_\lambda}\,[\text{count/photon}], \tag{1}$$

where all quantities are acquired by the calibration experiment, except the constant K. Therefore, we can only determine *relative* (not absolute) *spectral sensitivity* $C_{VIS}^{rel} = K\cdot C_{VIS}$ and $C_{NIR}^{rel} = K\cdot C_{NIR}$. Later we shall determine K and obtain an absolute sensitivity.

The presented calibration is done with the following parameters: Reflection on a protected aluminium mirror, integration time 0.5 s, slit-width 0.1 and 0.2 mm, number of averaged pixels 50 (H=5/V=10) and 1000 (H=10/V=100), respectively for VIS and NIR detection.[9] The obtained spectral sensitivity curves are shown in Fig. 3. The NIR sensitivity is quite flat while the VIS sensitivity increases toward short wavelengths where it is limited by the short-úass limit of the inverted dichroic beam-splitter.

IV. STANDARD SAMPLE AND ITS USE FOR ABSOLUTE CALIBRATION

Probably the most straightforward way to obtain an *absolute calibration* of the above derived *relative spectral sensitivity* is to measure an appropriate *standard sample* with well *characterized photoluminescence quantum yield* (PL QY) and its *spatial emission distribution*.

A potential standard sample has to fulfill several important requirements:

- Having the form of a thin layer (both physically and optically) in order to avoid problems with distribution of PL intensity in out-of-focus planes and reducing reabsorption and waveguiding effects.
- High PL QY value independent on excitation power (at least within certain range of excitation power).
- Broad PL spectrum located within a convenient wavelength range.

All article content, except where otherwise noted, is licensed under a Creative Commons Attribution 3.0 Unported license. See: http://creativecommons.org/licenses/by/3.0/ Downloaded to IP: 195.113.33.228 On: Mon, 20 Apr 2015 14:08:59

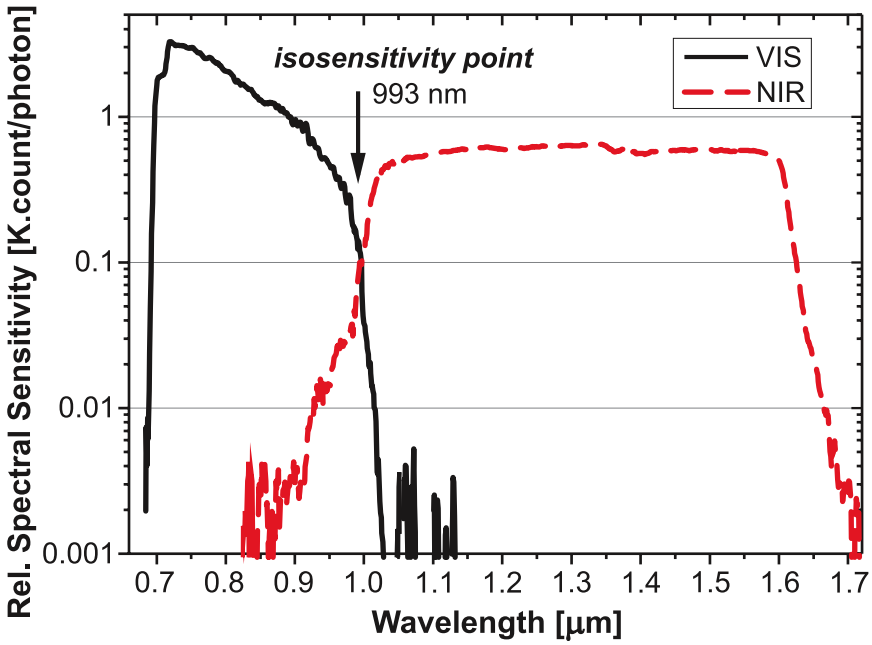

FIG. 3. Relative spectral sensitivity of the two parallel detection branches obtained using the 45 W tungsten lamp and reflection on an Al mirror.

- Spatial uniformity of PL properties (QY, excitation efficiency etc.).
- Perfect temporal- and photo-stability.
- Large Stokes shift between excitation and emission wavelength in order to reduce reabsorption.
- Excitation range matching some of the excitation bands available in the experimental apparatus.

We found that samples formed by a thin ***layer of Si nanocrystals*** (SiNCs) ***embedded in SiO$_2$*** fulfill most of the requirements for a standard sample. For this demonstration we have chosen a set of four samples formed by a luminescing layer deposited by the plasma-enhanced chemical-vapor deposition (PE-CVD) technique on a quartz substrate (25 × 25 mm) as a 200-nm thick monolayer of SiO_X (with the stoichiometry parameter x = 0.93, 1.05, 1.1, and 1.15) and subsequently annealed in N_2 at 1150 °C for 1 h and in H_2 at 500 °C for 1 h.[10] Normalized PL spectra of these samples are shown in Fig. 4(a) – the PL peak is conveniently placed between 930 and 1040 nm with FWHM of about 0.15 - 0.2 eV and the PL quantum yield is between 11 and 1 %. For the following tests we used sample Q3 (x = 1.05) with the PL peak around 1000 nm.

We have to note that thin luminescent layers have been already applied for microscopy calibration, e.g. Zwier et al.[11] described use of polymer layers with fluorescent dyes for luminescence microscopy image calibrations or recently Antonini et al.[12] described preparation of very thin fluorescent layers for characterization of axial resolution of sectioning microscopes.[13] However, there are probably no reports on the absolute microspectroscopy calibration using thin luminescing layers.

Characterization of the standard sample Q3 gives the following values of key parameters for excitation wavelength of 405 nm (3.0605 eV): Absorbance $A = 0.334$ and PL QY $\eta = 7$ %.[14] From the integral PL QY we can obtain spectral distribution of PL QY (Fig. 4(b)) via scaling of the measured PL spectrum. Such PL QY distribution represents probability that after absorption of one photon a PL photon is emitted at certain wavelength interval (1 nm wide). The integral of this spectrum must be equal to the measured total PL QY of 7 %.

For the absolute sensitivity calculation we must consider also the *angular distribution of PL emission* from the standard sample. It is expected that the emission pattern from a thin layer at an interface of two different media (here a silica glass and air) could deviate from the isotropic emission.[15] Therefore, the actual spatial distribution of PL must be characterized, for example by

All article content, except where otherwise noted, is licensed under a Creative Commons Attribution 3.0 Unported license. See: http://creativecommons.org/licenses/by/3.0/ Downloaded to IP: 195.113.33.228 On: Mon, 20 Apr 2015 14:08:59

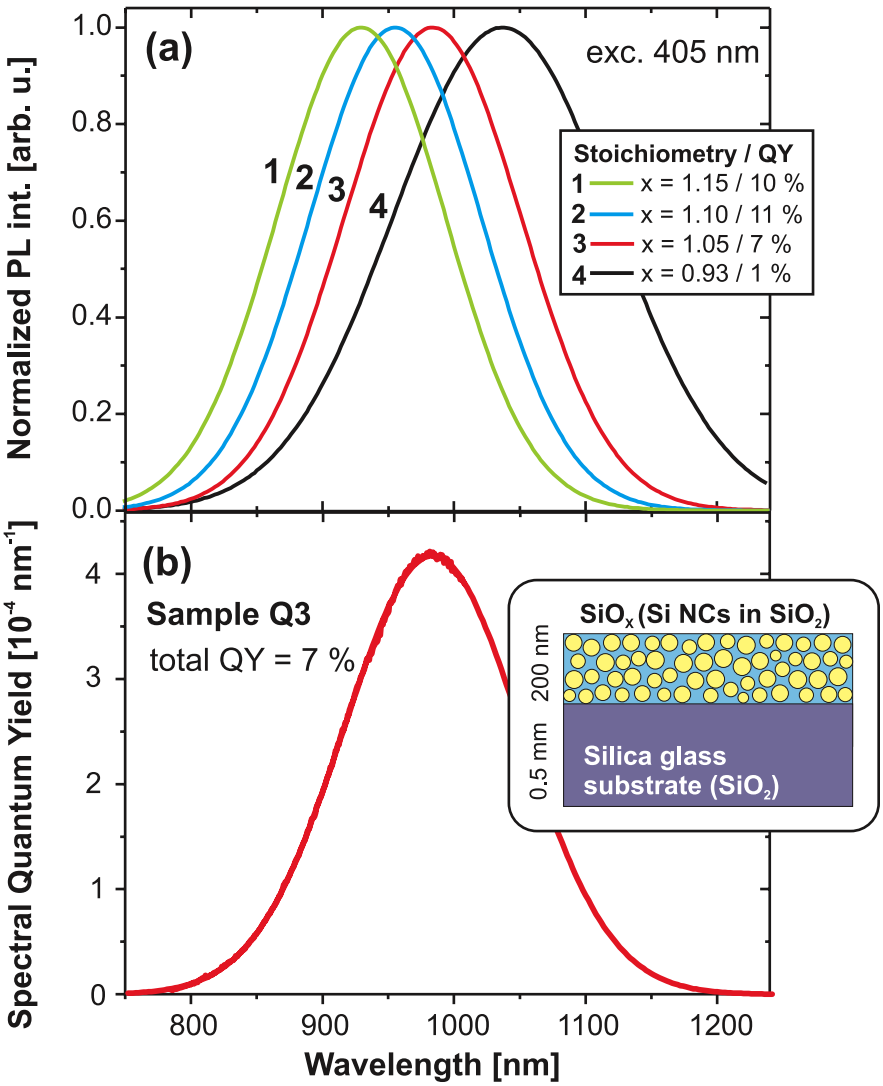

FIG. 4. (a) Normalized PL spectra of the SiNC samples. (b) The spectral quantum yield distribution for the sample Q3 determined in the integrating sphere set-up. The inset illustrates the standard sample structure.

measuring the angular distribution of PL with a goniometer set-up (see inset in Fig. 5). As the PL spectral shape is almost constant, we can plot either the integrated PL intensity or peak intensity (Fig. 5(a)) angle distribution (zero angle is the direction to the laser, the sample is perpendicular to this direction and the deposited SiO_X layer is facing the beam). It is clear (Fig. 5(a)), that more PL emission comes through the substrate (i.e. the medium with higher refraction index) as expected, but four local maxima observed at about 70°, 110°, 250°, and 290° are not well understood yet. The asymmetry of the left and right side of the PL angular distribution is probably due to imperfect symmetry of the goniometer set-up. The non-detectable part of the distribution (around 0° where the detecting fibre obscures the incoming laser beam) is replaced by the constant value of 0.5.

The collection efficiency for an objective lens with numerical aperture NA c_e is calculated as a spherical integral from 0° to arcsin(NA) divided by the total integrated emission. In Fig. 5(b) the experimental result is compared with the theoretical collection efficiency for an isotropic emitter. Due to a non-isotropic angular PL distribution of the standard sample, the objective lens with NA = 0.55 (applied in this work) has collection efficiency only c_e = 6 % (in contrast to 16.5 % for the Lambertian cosine emitter).

All article content, except where otherwise noted, is licensed under a Creative Commons Attribution 3.0 Unported license. See: http://creativecommons.org/licenses/by/3.0/ Downloaded to IP: 195.113.33.228 On: Mon, 20 Apr 2015 14:08:59

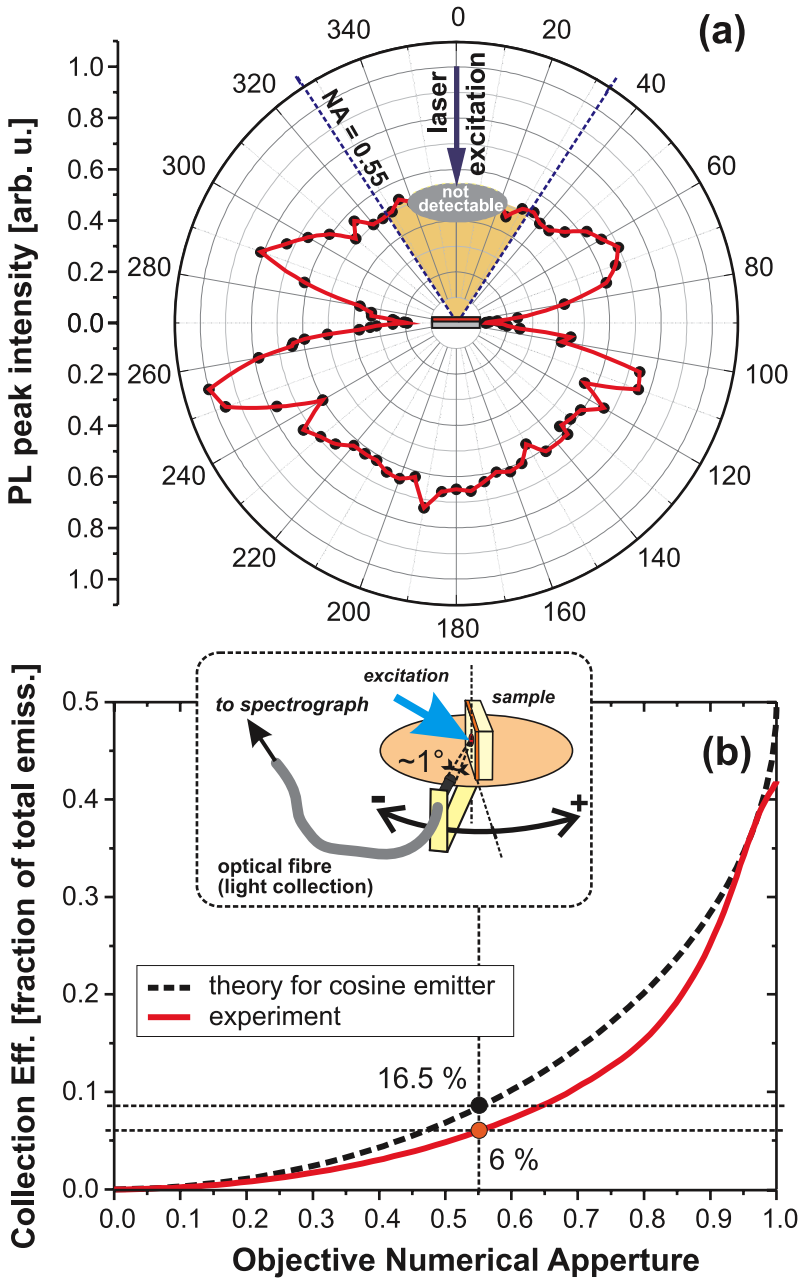

FIG. 5. (a) Angular distribution of PL peak emission from the sample Q3 excited perpendicularly by the 473-nm laser beam. SiNC layer is facing the beam. (b) Collection efficiency as function of numerical aperture. The dashed curve is a theoretical calculation for the cosine emitter and the solid curve is obtained by integrating the measured PL angular distribution (panel (a)).

The micro-PL spectra (VIS and NIR) of the standard sample were measured for different excitation intensities, in order to recognize a linear part of the PL excitation power dependence (Fig. 6(a)). PL saturation – deviation from the linear dependence of PL intensity on excitation power – starts already at power density of about 0.03 $W \cdot cm^{-2}$ (the typical value for SiNCs is 1 $W \cdot cm^{-2}$).[16] Then, any point from the linear part of the PL power dependence (Fig. 6(a)) can be chosen. Let us take the point corresponding to the excitation power of 15.4 $mW \cdot cm^{-2}$, i.e. 3.14×10^8 $photon \cdot s^{-1} \cdot \mu m^{-2}$ (incoming laser beam is attenuated by a filter with optical density OD = 3).

All article content, except where otherwise noted, is licensed under a Creative Commons Attribution 3.0 Unported license. See: http://creativecommons.org/licenses/by/3.0/ Downloaded to IP: 195.113.33.228 On: Mon, 20 Apr 2015 14:08:59

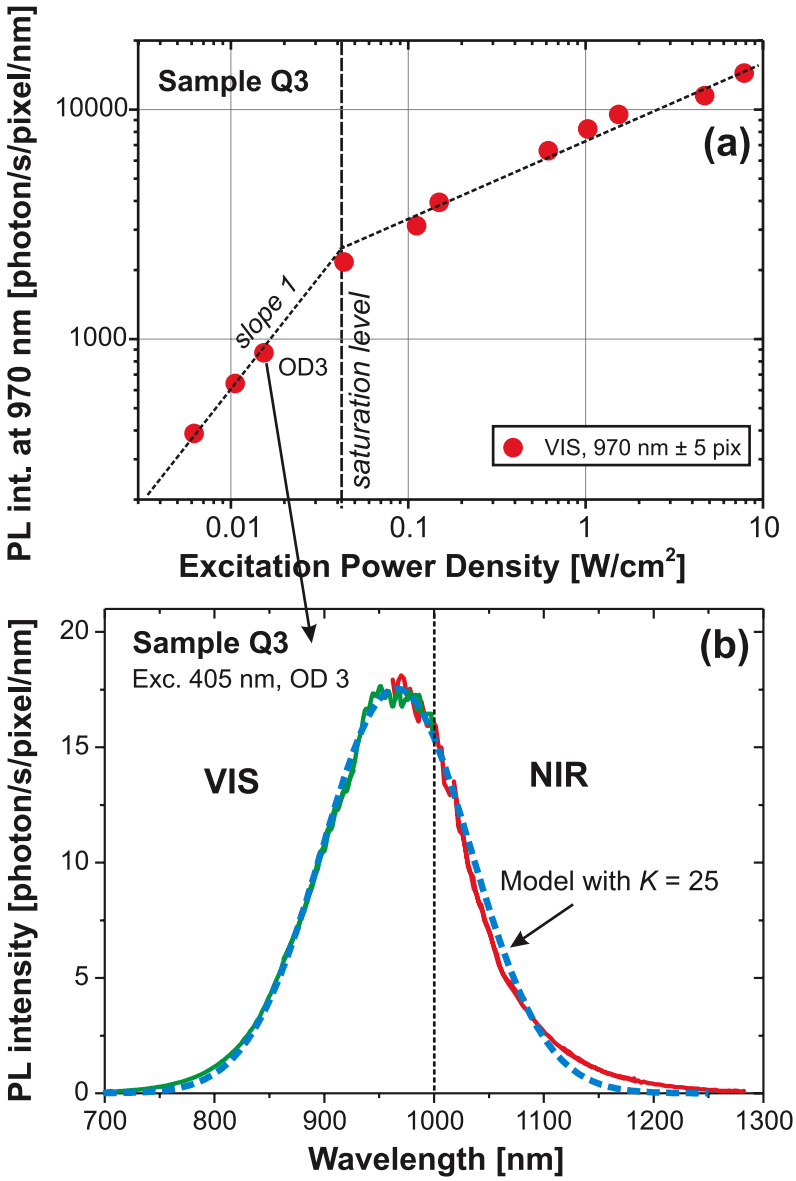

FIG. 6. (a) Excitation power dependence of PL signal from the standard sample at 970 nm. Only the excitation range below saturation, where PL is a linear function of excitation power density, is suitable for calibration purposes. (b) The spectral photon rate from the standard sample measured under 15 mW·cm^{-2} excitation (solid lines) compared with the spectrum (dashed line) calculated from the separately characterized properties of the standard sample. Close matching of the two spectra is possible by setting $K = 25$.

The absolute sensitivity calibration, i.e. determination of the constant K, is based on the following equation derived from Eq. (1)

$$C_{VIS/NIR} = \frac{C^{rel}_{VIS/NIR}}{K} = \frac{S^A_\lambda}{\Phi^a_{in}} = \frac{S^p/\Delta_\lambda}{I_{ex}\cdot\eta\cdot c_e\cdot A^p/M^2}, \tag{2}$$

where an *expected incoming photon irradiance* Φ_{in} from the standard sample is calculated from the excitation photon flux I_{ex} multiplied by absorbance A, PL QY η, coupling efficiency c_e, and the projected size of one pixel ($a = A^p/M^2 = 0.167$ μm^2). This gives the expected signal rate of 7.36×10^4 photon·s^{-1} per pixel. The value of K is then obtained by dividing this number by the measured PL signal with relative correction (i.e. divided by the relative spectral sensitivity).

All article content, except where otherwise noted, is licensed under a Creative Commons Attribution 3.0 Unported license. See: http://creativecommons.org/licenses/by/3.0/ Downloaded to IP: 195.113.33.228 On: Mon, 20 Apr 2015 14:08:59

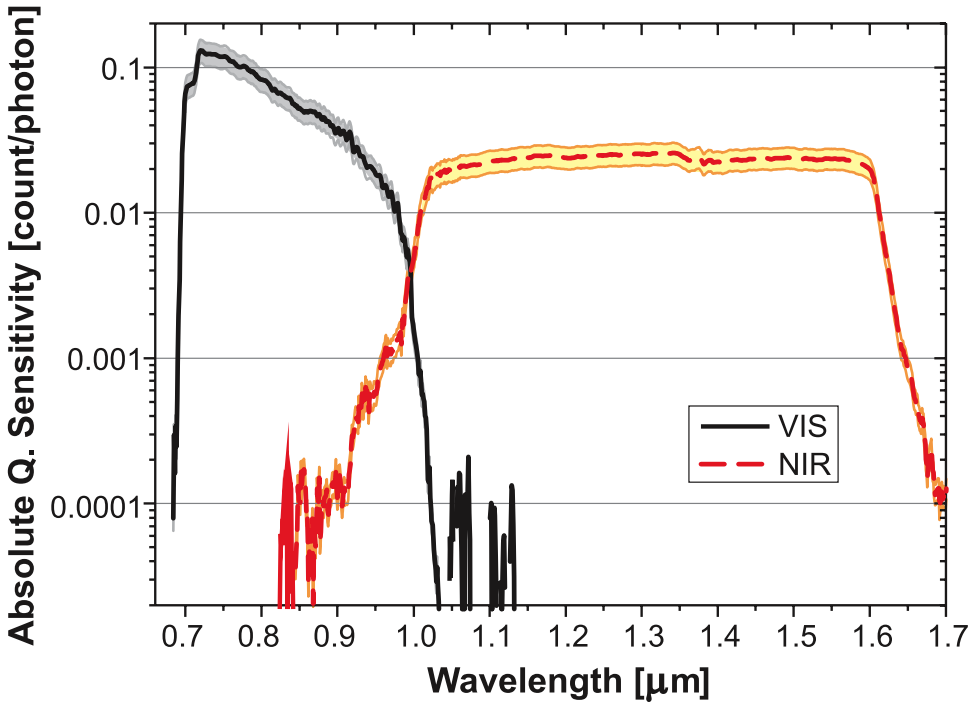

FIG. 7. Spectral sensitivity of the two spectroscope branches set to absolute scale by dividing data from Fig. 4 by K = 25. The shaded area corresponds to the estimated uncertainty of the absolute sensitivity.

This calculation is illustrated in Fig. 6(b), where the spectral distribution of the expected signal is calculated (dashed line) and fitted to the relatively-corrected experimental spectra (solid line) by adjusting the value of K to 25.

Finally, we divide the *relative spectral sensitivity* (Fig. 3) by $K = 25$ and obtain the desired ***absolute spectral sensitivity*** (Fig. 7). In order to estimate *uncertainty* of the derived absolute sensitivity values we take Eq. (2) and consider uncertainties only for variables in the denominator, so neglecting fluctuations of the measured spectral signal (i.e. the shot noise). The estimated relative uncertainties of photon flux I_{ex}, absorbance A, PL QY η, coupling efficiency c_e and the projected size of a pixel a, are 4 %, 2 %, 8 %, 10 %, and 1%, respectively. Applying the rules for propagation of errors in multivariable functions[17] we get the total relative uncertainty of 14 %. This is in fact a scaling error of the sensitivity (uncertainty of the parameter K) valid for the spectral region where the standard sample was measured. However, the broad sensitivity spectrum can be also "deformed" along its spectral axis and consequently the sensitivity uncertainty can increase with increasing spectral distance from the calibrated region. Let us estimate this effect as 1 % increase of relative uncertainty at spectral distance of 100 nm and plot the overall relative uncertainty in Fig. 7.

V. APPLICATION EXAMPLES

The absolute spectral sensitivity calibration, which relates the detected signal to the number of photons emitted from a sample, can be applied to derive external quantum yield of luminescing materials on the microscopy scale. We start from the following basic equation[1] for the photoluminescence intensity I_{PL} from an optically thin layer ($\alpha d << 1$)

$$I_{PL}(\lambda_{em}) = N \cdot I_{ex}(\lambda_{ex}) \cdot \sigma(\lambda_{ex}) \cdot \eta(\lambda_{ex}, \lambda_{em}), \quad (3)$$

where N is the areal density of absorbing centers, I_{ex} is excitation photon flux, σ is absorption cross section ($N \cdot \sigma = A$ is absorbance), and η is PL quantum yield, where λ_{ex} and λ_{em} are wavelengths of excitation and emission, respectively. The first three quantities on the right side of Eq. (3) give

All article content, except where otherwise noted, is licensed under a Creative Commons Attribution 3.0 Unported license. See: http://creativecommons.org/licenses/by/3.0/ Downloaded to IP: 195.113.33.228 On: Mon, 20 Apr 2015 14:08:59

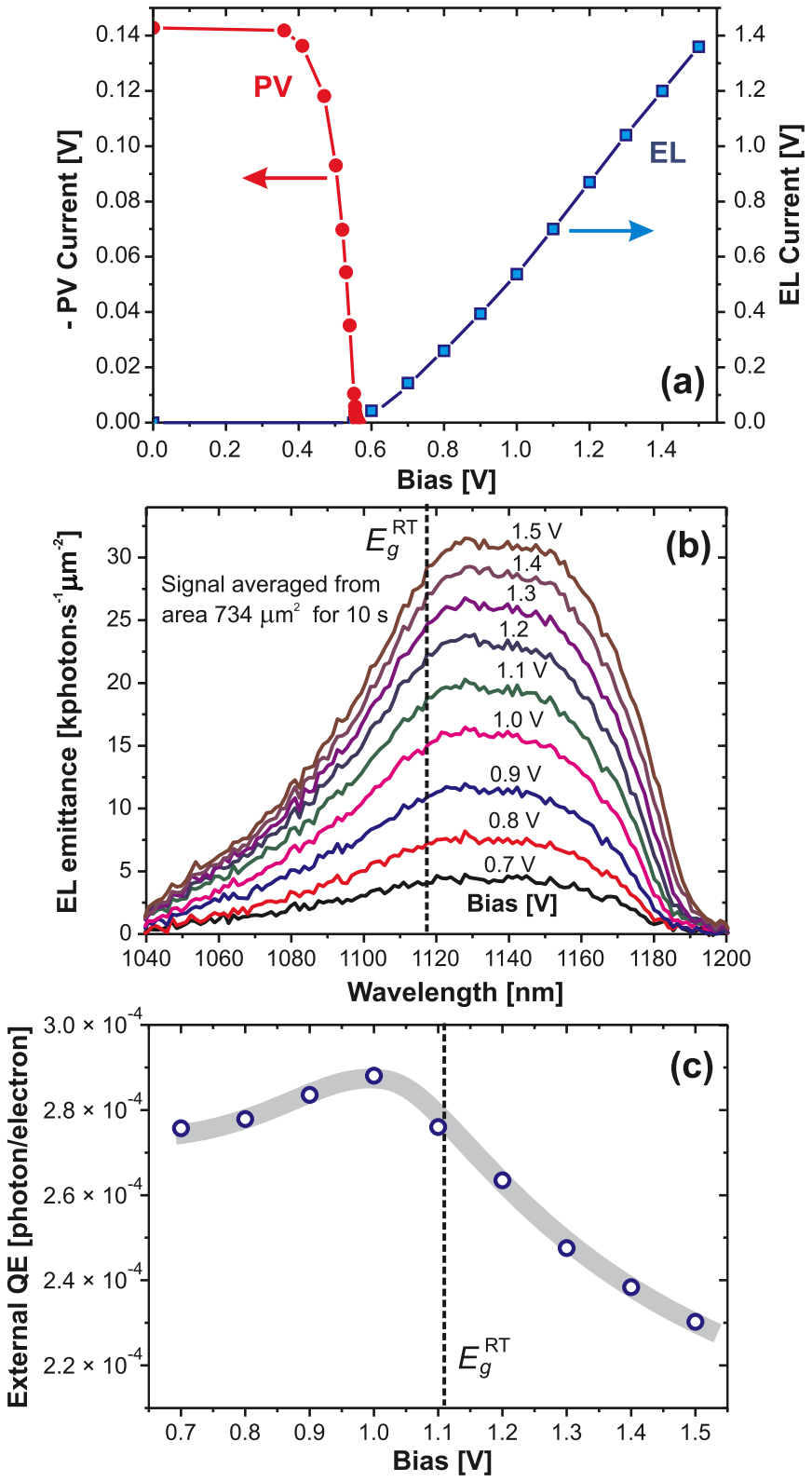

FIG. 8. (a) J-V characteristics of the poly-Si solar-cell under 1 Sun illumination (dots on the left side) and in darkness under externally applied bias during EL measurement (squares on the right side). (b) EL spectra under increasing bias converted to EL emittance using the absolute spectral sensitivity of the apparatus and assumption of the cosine angular distribution of EL emission in the upper hemisphere. (c) External quantum yield of EL emission as function of applied bias.

All article content, except where otherwise noted, is licensed under a Creative Commons Attribution 3.0 Unported license. See: http://creativecommons.org/licenses/by/3.0/ Downloaded to IP: 195.113.33.228 On: Mon, 20 Apr 2015 14:08:59

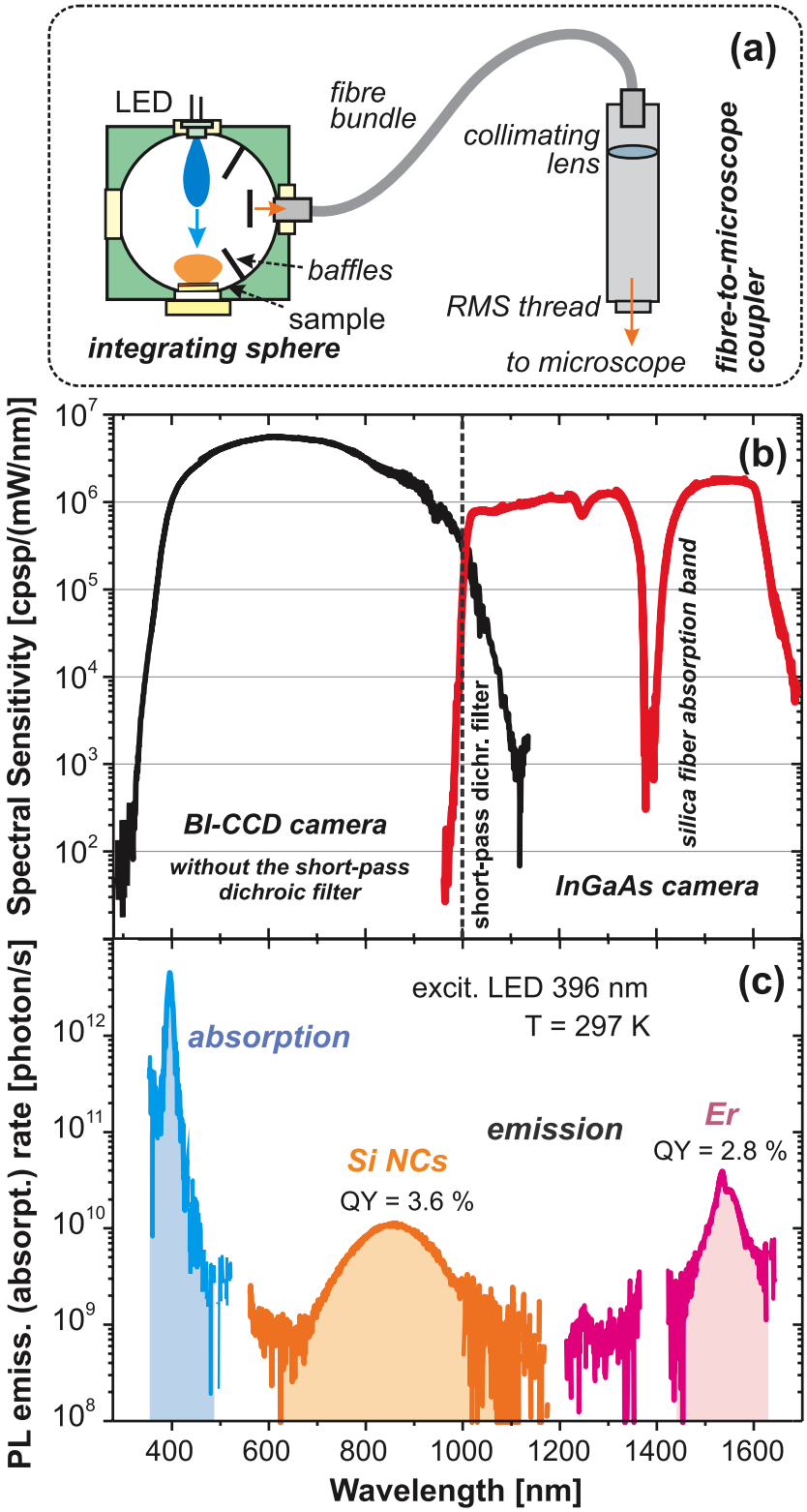

FIG. 9. (a) Schematical illustration of the integrating sphere set-up connected to the microspectroscope via a fiber bundle and an optical coupler (mounted on the objective thread). (b) Spectral sensitivity of the complete apparatus obtained as signal (in counts per second and per pixel - cpsp) divided by incoming spectral irradiance ($mW \cdot nm^{-1}$) entering the IS. The VIS detection is done without the short-pass dichroic filter. (c) PL emission and absorption rate of the SiNC:Er sample used for calculation of PL QY (QY value is indicated above each PL band).

All article content, except where otherwise noted, is licensed under a Creative Commons Attribution 3.0 Unported license. See: http://creativecommons.org/licenses/by/3.0/ Downloaded to IP: 195.113.33.228 On: Mon, 20 Apr 2015 14:08:59

absorption rate. While the incoming photon flux I_{ex} can be measured, N and σ must be determined or estimated separately. Also, for application of the absolute calibration to conversion of detected signal to I_{PL} one has to know or assume spatial distribution of emitted photons (directly related to the signal collection efficiency by an imaging lens).

One of the interesting applications of the above described set-up is characterization of solar-cells (SC) by their PL and EL (in case of silicon SCs their emission is situated between 1000 and 1200 nm, just matching the well calibrated spectral region). Advantage of EL external QY measurement is that number of emitted photons is related to current passing through a device which is easily measured. Therefore, only knowledge (or assumption) of EL spatial distribution is required for derivation of EL QY from detected micro-luminescence signal. EL characteristics are directly related to performance properties of a solar cell device[18] and can be effectively used for fast testing of SCs,[19] e.g. for determining minority carrier diffusion length.[20]

Here, we demonstrate the EL QY characterization of a small polycrystalline Si solar cell (SC) (Conrad Electronic SE, item No. 191254) with active area of 10×30 mm. The power efficiency under 1 Sun illumination (Solar simulator Newport Oriel Sol3A) of the tested SC is found to be about 5 % (J-V characteristics of this SC under 1 Sun illumination is shown in Fig. 8(a)). For EL characterization we mount SC in the above described microspectroscope and detect EL signal emitted from an area of 21 pixels (2.45 μm^2) under various DC bias (see Fig. 8). The measured EL intensity is converted to photon emittance using assumption of the cosine angular dependence of EL emission in the upper hemisphere.[21,22] Then the external EL QY (Fig. 8(c)) is obtained as ratio of emitted photons and number of passing elementary charges. The peak EQE value is around $(2.9 \pm 0.4) \cdot 10^{-4}$ which correspond well to literature data.[23]

Another example demonstrates usefulness of a relative sensitivity calibration over extremely broad spectral range for determination of external PL QY of Er-doped SiNCs. The tested sample is a thin layer of SiNCs in SiO_2 matrix deposited on a fused silica substrate by the radio-frequency magnetron co-sputtering of Si, SiO_2 and Er_2O_3, for details see Refs. 24 and 25. In order to make PL QY measurement independent on spatial distribution of PL emission the sample is placed in an integrating sphere (Fig. 9(a)). Excitation is done by the unfocused 396-nm LED and PL signal is collected by a silica fiber bundle whose output is coupled to the above described microspectroscope. A new relative spectral sensitivity (Fig. 9(b)) is measured for the whole apparatus including IS, the fiber bundle and the coupler (by illuminating the IS input port with the calibrated 45-W tungsten halogen filament lamp). The VIS detection branch is used without the inverted dichroic filter in order to enlarge detectable range down to ~350 nm. The NIR sensitivity dip around 1400 nm is due to absorption in the silica fiber bundle.

PL QY yield is derived from measurement of the SiNC:Er sample and a reference sample (bare substrate) by a procedure described in our recent paper.[7] Fig. 9(c) shows difference (absolute value) between signals from the tested sample and the reference sample converted to photon rate. QY of each PL emission band is then obtained as ratio of its integrated area (giving number of emitted photons) and the absorption band integrated area (number of absorbed photons). We get PL QY of (3.6 ± 0.3) % and (2.8 ± 0.2)% for the PL emission by SiNCs (around 850 nm) and by Er-dopants (around 1540 nm), respectively. The relative uncertainty is estimated (by the procedure described in Ref. 7,) to be ~8% which is much less than for the EL QY experiment (described above) as the IS-based experiment does not rely on the absolute but just the relative calibration. The extraordinary broad spectral range of this PL QY determination technique could be advantageous for studies of many materials, e.g. up-converting or down-converting luminescent materials.[26]

VI. CONCLUSIONS

We have proposed and tested a method of absolute calibration of a microspectroscope over an extraordinary broad spectral range covered by two (parallel) detection branches. The absolute calibration of a relative spectral sensitivity is performed using the standard sample formed by a thin layer of Si nanocrystals with stable photoluminescence around 1000 nm – the area where both detection branches overlap. The spectral PL quantum yield and the PL spatial distribution of

All article content, except where otherwise noted, is licensed under a Creative Commons Attribution 3.0 Unported license. See: http://creativecommons.org/licenses/by/3.0/ Downloaded to IP: 195.113.33.228 On: Mon, 20 Apr 2015 14:08:59

the standard sample were characterized by separate experiments. The relative uncertainty of the absolute calibration is estimated to be around 14 % but it can be reduced down to ~5 %.

This absolute calibration opens new applications of the optical microspectroscopy in quantitative characterization of various materials. For example, it enables us to calculate spectral photon emittance from a selected area of an investigated sample (even on the level of a single emitting nano-object like single molecule or quantum dot) entering the detection system (an objective lens). The total emittance could be estimated when the spatial distribution of PL of the studied sample (or object) is known – estimated or measured. Moreover, we can get also the emission QY if the absorbance (absorption cross section) is known. In the paper we demonstrate capabilities of this set-up by measuring external QY of electroluminescence from a standard poly-Si solar-cell and external QY of photoluminescence of Er-doped Si nanocrystals, where the broad VIS/NIR spectral range is necessary. We expect that the described method should find applications especially in the field of solar-cell materials or biomedical studies (detection of singlet oxygen emission at 1270 nm etc.).

The key component of our approach – the standard sample formed by a thin layer of luminescing Si nanocrystals in silica matrix - can be substituted by similar layers of efficiently luminescing materials (e.g. commercially available PbS quantum dots dispersed in PMMA and deposited by a spin coating an a glass substrate). In future, standard samples could be commercially supplied (including all necessary characterization data). The set-ups used in our calibration procedure may look quite complex but in fact all characterization of a standard sample can be performed using the same microspectroscopy set-up (providing the relative sensitivity was first measured with a radiation standard). Both the integrating sphere (for QY measurements, Fig. 9(a)) and the goniometer (for PL spatial distribution, Fig. 5(b)) can be assembled from standard optomechanical components and connected to a microscope via a fiber light-guide and a coupler (Fig. 9(a), also made from standard components).

ACKNOWLEDGEMENT

This work was performed within the framework of the Czech-Japan collaborative project Kontakt II 7E11021 (MSMT CR) and partially supported by the Bonus programme of Charles University. Authors are indebted to Prof. Zacharias' group at IMTEK, Freiburg, Germany for fabricating high-quality Si nanocrystalline layers used as calibration standards and also to group of Prof. Gregorkiewicz, University of Amsterdam, the Netherlands for providing Er-doped SiNC sample fabricated by D. Timmerman in the laboratory of Prof. Fujii, Kobe University, Japan.

[1] I. Pelant and J. Valenta, *Luminescence Spectroscopy of Semiconductors* (Oxford University Press, 2012).
[2] W. R. McCluney, *Introduction to Radiometry and Photometry* (Artech House Inc., Boston London, 1994).
[3] W.D. Niles and F.S. Cohen, Rev. Sci. Instr. **66**, 3527 (1995).
[4] J. Thigpen, F. A. Merchant, and S.K. Shah, J. Microscopy **239**, 200 (2010).
[5] Note, we recommend to avoid application of small spectrographs – having focal length shorter than about 25 cm – as they suffer from increasing stray light intensity which significantly affects results of sensitivity calibration obtained by measuring broad-band light sources. The stray-light-effects are strong in spectral regions where sensitivity drops down).
[6] J. Valenta, R. Juhasz, and J. Linnros, J. Luminescence **98**, 15 (2002).
[7] J. Valenta, Nanosci. Methods **3**, 11 (2014).
[8] I. Pelant, T. Ostatnický, J. Valenta, K. Luterová, E. Skopalová, T. Mates, and R.G. Elliman, Appl. Phys. B **83**, 87 (2006).
[9] Note, the number of pixels over which signal was averaged is different from the 3x2 pixels in the schematical illustration on Fig. 2. In fact, the result of the described procedure should be independent on the number of averaged pixels; unless the signal distribution changes significantly within the averaged area (such situation must be avoided not only during calibration but also during all subsequent measurements). It means that one can adapt number of averaged pixels and a slit width (within certain limits) in order to improve signal-to-noise ratio.
[10] A. M. Hartel, D. Hiller, S. Gutsch, P. Löper, S. Estradé, F. Peiró, B. Garrido, and M. Zacharias, Thin Solid Films **520**, 121 (2011).
[11] J.M. Zwier, G.J. van Rooij, J.W. Hofstraat, and G.J. Brakenhoff, J. Microscopy **216**, 15 (2004).
[12] A. Antonini, C. Liberale, and T. Fellin, Opt. Express **22**, 14293 (2014).
[13] G.J. Brakenhoff, G.W.H. Wurpel, K. Jalink, L. Oomen, L. Brocks, and J.M. Zwier, J. Microscopy **219**, 122 (2005).
[14] J. Valenta, M. Greben, S. Gutsch, D. Hiller, and M. Zacharias, Appl. Phys. Lett. **105**, 243107 (2014).
[15] H.E. Hellen and D. Axelrod, J. Opt. Soc. Am **4**, 337 (1987).
[16] J. Valenta, A. Fucikova, F. Vácha, F. Adamec, J. Humpolíčková, M. Hof, I. Pelant, K. Kůsová, K. Dohnalová, and J. Linnros, Adv. Functional Materials **18**, 2666 (2008).

All article content, except where otherwise noted, is licensed under a Creative Commons Attribution 3.0 Unported license. See: http://creativecommons.org/licenses/by/3.0/ Downloaded to IP: 195.113.33.228 On: Mon, 20 Apr 2015 14:08:59

[17] I.G. Hughes and T.P.A. Hase, *Measurements And Their Uncertainties: A Practical Guide to Modern Error Analysis* (Oxford University Press, Oxford, 2010).
[18] U. Rau, Phys. Rev. B **76**, 085303 (2007).
[19] T. Fuyuki and A. Kitiyanan, Appl. Phys. A **96**, 189 (2009).
[20] P. Würfel, T. Trupke, T. Puzzer, E. Schäffer, W. Warta, and S.W. Glunz, J. Appl. Phys. **101**, 123110 (2007).
[21] This assumption may be quite rough, but the purpose of this experiment is just to demonstrate application potential of the calibrated VIS/NIR microspectroscope for SC testing via EL yield determination. If necessary, the angular distribution of EL from a SC can be characterized using the goniometer set-up as shown in Fig. 5 (but without the excitation laser).
[22] T. Trupke, E. Dayb, and P. Würfel, Sol. En. Mater. & Sol. Cells **53**, 103 (1996).
[23] T. Kirchartz, A. Helbig, W. Reetz, M. Reuter, J. H. Werner, and U. Rau, Prog. Photovolt: Res. Appl. **17**, 394 (2009).
[24] M. Fujii, M. Yoshida, Y. Kanzawa, S. Hayashi, and K. Yamamoto, Appl. Phys. Lett. **71**, 1198 (1997).
[25] I. Izzedin, D. Timmerman, T. Gregorkiewicz, A.S. Moskalenko, A.A. Prokofiev, I.N. Yassievich, and M. Fujii, Phys. Rev. B **78**, 035327 (2008).
[26] J. Zhao, D. Jin, E.P. Schartner, Y. Lu, Y. Liu, A.V. Zvyagin, L. Zhang, J. M. Dawes, P. Xi, J.A. Piper, E.M. Goldys, and T.M. Monro, Nature Nanotech. **8**, 729 (2013).

All article content, except where otherwise noted, is licensed under a Creative Commons Attribution 3.0 Unported license. See: http://creativecommons.org/licenses/by/3.0/ Downloaded to IP: 195.113.33.228 On: Mon, 20 Apr 2015 14:08:59